Formation, Properties, and Characterization of a Fully Reduced $Fe^{II}Fe^{II}$ Form of Spinach (and Parsley) [2Fe-2S] Ferredoxin with the Macrocyclic Complex $[Cr(15\text{-ane}N_4)(H_2O)_2]^{2+}$ as Reductant

Sang-Choul Im,[†] Takamitsu Kohzuma,[†] William McFarlane,[†] Jacques Gaillard,[‡] and A. Geoffrey Sykes*,[†]

Department of Chemistry, University of Newcastle, Newcastle upon Tyne NE1 7RU, U.K., and CEA, DRFMC/SCIB/SCPM, 17 rue des Martyrs, 30054 Grenoble Cedex 9, France

Received July 12, 1996[⊗]

Reduction of spinach and parsley ferredoxin FdI in the $Fe^{III}Fe^{III}$ state with the 1,4,8,12-tetraazacyclopentadecane complex $[Cr(15\text{-ane}N_4)(H_2O)_2]^{2+}$, here written as $Cr^{II}L$, provides the first evidence for two 1-equiv steps yielding an $Fe^{II}Fe^{II}$ product. Rate constants (25 °C) for spinach FdI are 2760 and 660 M^{-1} s^{-1}, respectively, at pH 7.5, $I = 0.100$ M (NaCl). An important observation is that the $Cr^{III}L$ generated in the first step remains attached to the $Fe^{II}Fe^{III}$ product and perturbs the protein active site sufficiently to make the second stage possible. The second $Cr^{II}L$ reduction is of the "outer-sphere" type, and the $Cr^{III}L$ generated is not attached to the protein. Anaerobic reoxidation of the fully reduced protein with $[Co(NH_3)_6]^{3+}$ is rapid and can be achieved with ∼80% recovery of the $Fe^{III}Fe^{III}$ oxidation state over 40 min. Air oxidation yields the $Cr^{III}L$ product $Fe^{III}Fe^{III}\cdots Cr^{III}L$ (Fe:Cr = 2:1). With *Anabaena variabilis* only a one-step reduction is observed and there is no $Cr^{III}L$ attachment. From a comparison of amino acid sequences with spinach (and parsley) FdI, a likely point of $Cr^{III}L$ attachment is indicated. Comparisons are made with dithionite as reductant. In addition, square-wave voltammetry on spinach $Fe^{III}Fe^{III}\cdots Cr^{III}L$ gives two reduction potentials −273 and −410 mV vs NHE. The different redox products have been characterized by EPR. Using ^1H NMR line-broadening techniques, evidence for $Cr^{III}L$ binding at a surface site close to Tyr-25/Tyr-82 is obtained. Also from investigations with redox-inactive $[Cr(en)_3]^{3+}$ as a competitive inhibitor for $Cr^{II}L$ reduction of spinach $Fe^{III}Fe^{III}$, Tyr-25/Tyr-82 is proposed as the site for $Cr^{II}L$ reduction. From an extension of studies to include reduction of $Fe^{III}Fe^{III}\cdots Cr^{III}L$ with $Cr^{II}L$, evidence is obtained for a second reaction site when that at Tyr-25/Tyr-82 is no longer available.

Introduction

The [2Fe-2S] ferredoxins (M_r = ∼10 500; 93−99 amino acids) are an important class of redox metalloproteins found in the leaves of higher plants and in algae.[1,2] The ferredoxins are involved in processes as diverse as photosynthesis, nitrite reductase, sulfite reductase, glutamate synthesis, nitrogen fixation, thioredoxin oxidoreduction, and lipid desaturation.[3−5] It is now established that many plant (leaf) and algal sources have at least two different [2Fe-2S] molecules present. A distinction between the iso forms on the basis of their functionality has not so far been possible.[6] The [2Fe-2S] ferredoxins are very acidic, pI values from 3 to 4, with charge balance −18 (±2) at pH ∼7.5 from amino acid compositions. There are now over 75 amino acid sequences of the protein from higher plants and algae (prokaryotic and eukaryotic).[7] Five X-ray crystal structures for the $Fe^{III}Fe^{III}$ state from blue-green algal (cyanobacteria) sources *Spirulina platensis*,[8] *Aphanothece sacrum*,[9] *Anabaena* 7120,[10] *Halobacterium* of the Dead Sea,[11] and *Equisetum arvense*[12] (resolutions 1.7−2.5 Å) have been reported. The active site consists of two bis(μ-sulfido)-bridged high-spin tetrahedral Fe^{III} atoms ($S = {}^5/_2$), which are antiferromagnetically coupled and therefore EPR silent.[13] The binuclear Fe core is coordinated to four cysteines (RS^-) at positions 41, 46, 49, and 79 to give $[Fe_2S_2(SR)_4]^{2-}$ in the three [2Fe-2S] proteins considered in this paper. Reduction potentials for the one-electron redox process (1) are in the range −430 ± 20 mV.[14]

$$Fe_2S_2^{2+} + e^- \rightleftarrows Fe_2S_2^{+} \qquad (1)$$

No previous evidence for reduction to the $Fe^{II}Fe^{II}$ state has been obtained even under strongly reducing electrochemical conditions. One of the metal atoms Fe_A is closer to the surface (∼5 Å), and the Cys-41 and Cys-46 residues bonded to it are partially exposed. Although there is no crystal structure for the $Fe^{II}Fe^{III}$ state, it has been demonstrated by NMR that the extra electron is localized on Fe_A.[15]

[†] CEA.
[‡] University of Newcastle.
[⊗] Abstract published in *Advance ACS Abstracts,* February 15, 1997.

(1) Matsubara, H.; Saeki, K. *Adv. Inorg. Chem.* **1992**, *38*, 223−280.
(2) Cammack, R. *Adv. Inorg. Chem.* **1992**, *38*, 281−322.
(3) Arnon, D. I. *Trends Biochem. Sci.* **1988**, *13*, 30.
(4) Crawford, N. A.; Yee, B. C.; Droux, M.; Carlson, D. E.; Buchanan, B. B. In *Methods in Enzymology;* Packer, L., Glazer, A. N., Eds.; Academic Press: San Diego, CA, 1988; Vol. 167, p 415.
(5) Schmidt, H.; Heinz, E. *Plant Physiol.* **1990**, *94*, 214.
(6) Wada, K.; Ohoka, H.; Matsubara, H. *Physiol. Veg.* **1985**, *23*, 679.
(7) See ref 1, p 225, for details.
(8) Tsukihara, T.; Fukuyama, K.; Nakamura, M.; Katsube, Y.; Tanaka, N.; Kakudo, M.; Wada, K.; Hase, T.; Matsubara, H. *J. Biochem.* **1981**, *90*, 1763.
(9) Tsukihara, T.; Fukuyama, K.; Mizushima, M.; Harioka, T.; Kusunoki, M.; Katsube, Y.; Hase, T.; Matsubara, H. *J. Mol. Biol.* **1990**, *216*, 399.
(10) (a) Rypniewski, W. R.; Breiter, D. R.; Benning, M. M.; Wesenberg, G.; Oh, B.-H.; Markley, J. L.; Rayment, I.; Holden, H. M. *Biochemistry* **1991**, *30*, 4126. (b) Jacobson, B. L.; Chae, Y. K.; Markley, J. L.; Rayment, I.; Holden, H. M. *Biochemistry* **1993**, *32*, 6788.
(11) Sussman, J. L.; Shoham, M.; Hazel, M. *Prog. Clin. Biol. Res.* **1989**, *289*, 171.
(12) Ikemizu, S.; Fukuyama, K. *Acta Crystallogr.* **1994**, *D50*, 167.
(13) Hase, T.; Matsubara, H. *J. Mol. Biol.* **1981**, *90*, 1763.
(14) (a) Tagawa, K.; Arnon, D. I. *Biochim. Biophys. Acta* **1968**, *153*, 602. (b) Salamon, Z.; Tollin, G. *Bioelectrochem. Bioenerg.* **1992**, *27*, 381.
(15) Dugad, L. B.; La Mar, G. N.; Banci, L.; Bertini, I. *Biochemistry* **1990**, *29*, 2263.

S0020-1669(96)00825-7 CCC: $14.00 © 1997 American Chemical Society

Two isoferredoxins FdI and FdII (in order of elution) have been isolated from spinach, parsley, and *A. variabilis*,[16] and the reactivity of the major FdI components has been explored. It has been shown in the case of spinach that the two forms have a substantial number of amino acids (25) which are different.[17] In spite of this, the two forms exhibit similar reactivities with $[Co(NH_3)_6]^{3+}$ and $[Cr(phen)_3]^{3+}$ as oxidants for the $Fe^{II}Fe^{III}$ state.[18] The reactivity of spinach FdI with the Cr^{II}-macrocycle complex $[Cr(15\text{-}aneN_4)(H_2O)_2]^{2+}$, referred to here as $Cr^{II}L$, where 15-$aneN_4$ is the saturated 1,4,8,12-tetraazacyclopentadecane ligand, provides the main focus in this study. The structure of $[Cr(15\text{-}aneN_4)(NCS)(H_2O)]^{2+}$ has been determined and indicates a trans structure.[19] The product $[Cr(15\text{-}aneN_4)(H_2O)_2]^{3+}$ has pK_a (25 °C) values of 2.9 and 7.8 corresponding to the H_2O ligand acid dissociation constants.[20] The $Cr^{III}L/Cr^{II}L$ couple has a reduction potential of −580 mV at $[H^+] = 0.40$ M.[21] Comparisons with parsley and *A. variabilis* FdI are made. Absorbance changes are consistent with reactions proceeding further than the $Fe^{II}Fe^{III}$ state and two well-defined redox steps. A communication reporting the initial parsley FdI findings has appeared.[22] More extensive characterizations of the reactions and products obtained, as well as evidence for involvement of a second redox site on the protein when the first is not available, form a part of the present studies.

Experimental Section

Protein Isolation. Procedures for the isolation of [2Fe-2S] ferredoxins from fresh spinach and parsley leaves have been reported.[16] *Anabaena variabilis* blue-green algae (cyanobacteria) were grown in 20 L vessels at ∼30 °C over ∼3 days, harvested, and stored frozen after filtration.[23,24] Samples of [2Fe-2S] were stored as the $Fe^{III}Fe^{III}$ protein at −20 °C under N_2. The purity was checked using ratios of UV−vis absorbance at 422 and 278 nm. Ratios A_{422}/A_{278} (FdI and FdII mixture) obtained for spinach, >0.46 (in this work 0.49), for parsley, >0.60 (0.62), and *A. variabilis*, >0.58 (0.60), were used as a check of purity.[18]

Separation of FdI and FdII Components. A phenyl superose HR 5/5 hydrophobic column attached to a Pharmacia FPLC system was used.[25] All buffers were made air-free with N_2 before use to minimize loss of ferredoxins. The buffers used for separation were, in solution A, 20 mM Tris/HCl at pH 7.5 and, in solution B, 20 mM Tris/HCl containing 1.7 M ammonium sulfate at pH 7.5. The column was equilibrated in buffer B, and the protein sample was loaded into this same buffer. Separation was achieved using a linear gradient (1.75%/cm^3) of 0−50% A with a flow rate of 0.5 cm^3 min^{-1}. Elution was monitored at 280 nm using a UV-M control. Major (FdI) and minor (FdII) components were separated in ratios of 84% FdI to 16% FdII (spinach), 70% FdI to 30% FdII (parsley), and 92% FdI to 8% FdII (*A. variabilis*).

Buffer. Solutions of tris(hydroxymethyl)methylamine (Trizma) were used, here referred to as Tris (Sigma Chemicals), with dilute HCl added to give pH's in the range 7−9 as required. A Radiometer PHM62 meter was used to measure pH. The ionic strength of solutions was adjusted to $I = 0.100$ M with NaCl.

Complexes. A sample of chromium(II) chloride, $CrCl_2 \cdot 4H_2O$, was prepared anaerobically by a literature method.[26] Required amounts of the ligand 1,4,8,12-tetraazacyclopentadecane (Strem Chemicals), 15-$aneN_4$, were added to $CrCl_2 \cdot 4H_2O$ in Tris/HCl buffer, to give $[Cr(15\text{-}aneN_4)(H_2O)_2]^{2+}$, $I = 0.10$ M (NaCl). Rigorous air-free techniques using a Miller-Howe glovebox (O_2 <2 ppm) were required at all times. Over the pH range investigated, the $Cr^{II}L$ complex gives a UV−vis absorbance peak at 540 nm ($\epsilon = 36.5$ M^{-1} cm^{-1}). On air oxidation at pH 1.5, the $Cr^{III}L$ product $[Cr(15\text{-}aneN_4)(H_2O)_2]^{3+}$ is formed; peak positions λ/nm (ϵ/M^{-1} cm^{-1}) at 377 (88) and 454 (87) as previously reported.[20] Concentrations of $Cr^{II}L$ were also determined by addition to $[IrCl_6]^{2-}$; peak position λ/nm (ϵ/M^{-1} cm^{-1}) 487 (4075).[27]

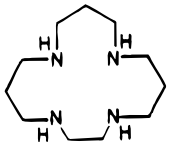

15-aneN$_4$

A sample of tris(ethylenediamine)chromium(III), $[Cr(en)_3]Cl_3 \cdot 3H_2O$, peak positions λ/nm (ϵ/M^{-1} cm^{-1}) 351 (63) and 457 (73), was prepared as described.[28]

Preparation and Metal Content of Cr-Modified [2Fe-2S] Protein. Addition of a 2.4:1 excess of $Cr^{II}L$ to [2Fe-2S] ferredoxin $Fe^{III}Fe^{III}$, followed by (rapid) air oxidation, DE52 column separation, and purification by Mono-Q Pharmacia FPLC anion exchange column chromatography, gave a $Cr^{III}L$-attached product written as $Fe^{III}Fe^{III}\cdots Cr^{III}L$, referred to also as $Cr^{III}L$-modified protein. The product is stable at 25 °C under anaerobic conditions. Metal analyses carried out by inductively coupled plasma atomic emission spectroscopy (ICP-AES) gave Cr:Fe ratios of 1:2.0 (spinach) and 1:2.2 (parsley). The Cr content was also determined by a colorimetric method. This involved addition of 9 M H_2SO_4 and oxidizing with ammonium persulfate (reflux ∼20 min). Excess diphenylcarbazide solution was added to give the Cr^{VI}−diphenylcarbazide product peak at 540 nm (ϵ 31 000 M^{-1} cm^{-1}).[29]

Other Reagents. Sodium dithionite, $Na_2S_2O_4$ (Fluka Chemicals), was standardized spectrophotometrically using the $[Fe(CN)_6]^{3-}$ peak at 420 nm (ϵ 1010 M^{-1} cm^{-1}). Samples used were found to be ∼86% pure. Using glovebox techniques, it was found that ∼1 mM solutions of dithionite could be prepared quantitatively.

Kinetic Studies. Reactions at 25.0 ± 0.1 °C were monitored using the $Fe^{III}Fe^{III}$ ferredoxin absorbance peak at 422 nm, which gives a $\Delta\epsilon$ = 4900 M^{-1} cm^{-1} decrease on one-electron reduction to the $Fe^{II}Fe^{III}$ state.[30] A Dionex D110 stopped-flow spectrophotometer and a fitting procedure from On-Line Instrument Systems (OLIS, Bogart, GA) were used. Biphasic kinetic fits were used as appropriate. Rate constants reported are an average of at least five stopped-flow traces for the same reactant solutions. Tris buffer concentrations employed were 20 mM.

Electrochemistry. Square-wave voltammetry measurements were carried out using a standard three-electrode configuration of gold, Ag/AgCl, and platinum as working and reference electrodes, respectively, in conjunction with a Princeton Applied Research Model 173 potentiostat interfaced to an IBM PC computer with software from EG&G. The gold electrode was hand-polished using in turn 0.03 and 0.15 μm aqueous aluminum oxide slurries as polishing material (Böehler) and cleaned by sonication for 30 s. The electrode was modified by soaking in a solution of the promoter 2-(diethylamino)ethyl mercaptan (DEAE-SH) (Sigma), which gave a positively charged surface suitable for an acidic protein.[31] The procedure was tested first using native spinach FdI. A peak at −462 mV vs NHE was obtained for native spinach [2Fe-2S] ferredoxin, agreeing with a previous value[32] but more negative

(16) (a) Armstrong, F. A.; Henderson, R. A.; Sykes, A. G. *J. Am. Chem. Soc.* **1979**, *101*, 6912. (b) Lloyd, E.; Tomkinson, N. P.; Salmon, G. A.; Sykes, A. G. *Biochim. Biophys. Acta* **1993**, *1202*, 113.
(17) Takahasi, Y.; Hase, T.; Wada, K.; Matsubara, H. *Plant Cell Physiol.* **1983**, *24*, 189.
(18) Lloyd, E.; Tomkinson, N. P.; Sykes, A. G. *J. Chem. Soc., Dalton Trans.* **1992**, 753.
(19) Clegg, W.; Leupin, P.; Richens, D. T.; Sykes, A. G.; Roper, E. S. *Acta Crystallogr.* **1985**, *C41*, 530.
(20) Richens, D. T.; Adzamli, I. K.; Leupin, P.; Sykes, A. G. *Inorg. Chem.* **1984**, *23*, 3065.
(21) Samuels, G. J.; Espenson, J. H. *Inorg. Chem.* **1979**, *18*, 2587.
(22) Im, S.-C.; Lam, K.-Y.; Lim, M.-C.; Ooi, B.-L.; Sykes, A. G. *J. Am. Chem. Soc.* **1995**, *117*, 3635.
(23) Jackman, M. P.; Sinclair-Day, J. D.; Sisley, M. J.; Sykes, A. G.; Denys, L. A.; Wright, P. E. *J. Am. Chem. Soc.* **1987**, *109*, 6443.
(24) Kratz, W. A.; Meyers, J. *Am. J. Bot.* **1955**, *42*, 282.
(25) Sakihama, N.; Shin, M.; Toda, H. *J. Biochem.* **1986**, *100*, 43.
(26) Holah, D. G.; Fackler, J. P., Jr. *Inorg. Synth.* **1969**, *10*, 26.
(27) Sykes, A. G.; Thorneley, R. N. F. *J. Chem. Soc. A* **1969**, 655.
(28) Gillard, R. D.; Mitchell, P. R. *Inorg. Synth.* **1972**, *14*, 184.
(29) (a) Ege, J.; Silverman, L. *Anal. Chem.* **1947**, *19*, 693. (b) Sandell, E. B. in *Colorimetric Determination of Traces of Metals*, 3rd ed.; Interscience: New York, 1959; pp 392−397.
(30) Fee, J. A.; Mayhew, S. G.; Palmer, G. *Biochim. Biophys. Acta* **1971**, *245*, 196.
(31) Guo, L.-H.; Hill, H. A. O. *Adv. Inorg. Chem.* **1991**, *36*, 341−375.

than values close to −430 mV determined by procedures not involving a promoter.[33−35] Only a single redox process is observed. With the $Cr^{III}L$-modified protein, the same procedure was adopted and two well-defined peaks were observed.

EPR Spectra. These were recorded on an X-band Varian E-109 spectrometer. An Oxford Instruments EPR 900 helium-flow cryostat was used to adjust the sample temperature to 10 K with a microwave power of 0.01 mW. Quantification of the spin concentration was performed by double integration and comparison with a purified sample of *C. pasteurianum* [2Fe-2S] ferredoxin of known concentration.[36] Other experimental conditions: microwave frequency, 9.230 GHz; modulation amplitude, 1 mT. Solutions of spinach FdI were reduced by dithionite and $Cr^{II}L$ at pH 7.0 (20 mM Tris/HCl), $I = 0.100$ M (NaCl).

NMR Spectra. Samples were prepared in D_2O (99.9%) at pH 7.5 uncorrected for D_2O (50 mM phosphate) using ultrafiltration methods (Amicon; YM5 membrane). Concentrations of $Fe^{III}Fe^{III}$ and Fe^{III}-$Fe^{III}\cdots Cr^{III}L$ (1.5−2.0 mM) were determined by UV−vis spectrophotometry at 422 nm (ϵ 9200 M^{-1} cm^{-1}). The pH values of solutions in an NMR tube were determined using a narrow CMAWL/3.7/180 pH probe (Russell) in combination with a Radiometer PHM62 pH meter. After the protein solution was loaded into an NMR tube (5 mm o.d. borosilicate glass), the tube was flushed with argon and sealed. All ^1H NMR spectra were acquired at 500.14 MHz on a Bruker AMX500 spectrometer (25 °C). For one-dimensional spectra, free induction decays were accumulated into 16K data points and transferred into 32K data points after zero-filling. The residual HDO resonance was suppressed by presaturation at its resonance frequency. All chemical shifts are cited in parts per million (ppm) relative to HDO at δ 4.81. Two-dimensional NMR techniques NOESY and TOCSY were employed. The mixing times for NOESY experiments were 50−250 ms, and the mixing time for the TOCSY experiments was 34 ms.

Results

Kinetic Studies on the $Cr^{II}L$ Reduction of FdI. Spinach (and parsley[22]) FdI in the $Fe^{III}Fe^{III}$ state give biphasic stopped-flow kinetics on reduction with $Cr^{II}L$, and absorbance changes (422 nm) are consistent with the reaction proceeding further than the $Fe^{II}Fe^{III}$ stage. Earlier reports[37] that, with $S_2O_4^{2-}$, the only product is $Fe^{II}Fe^{III}$, (2), were confirmed. The final spectrum following reduction with 2 equiv of $Cr^{II}L$ is shown alongside spectra of $Fe^{III}Fe^{III}$ and $Fe^{II}Fe^{III}$ forms in Figure 1A. The inset illustrates the biphasic nature of absorbance changes monitored at 422 nm. The product was allowed to air-oxidize when the column-purified protein gave the same UV−vis spectrum as that of native $Fe^{III}Fe^{III}$, and analyses gave a 2:1 Fe:Cr content , consistent with (3). No contributions to final spectra of $Cr^{III}L$ (or $Cr^{II}L$), which are relatively weakly absorbing, were observed. Different behavior was observed for $Fe^{III}Fe^{III}$ *A. variabilis* FdI with excess $Cr^{II}L$, which gave Fe^{II}-Fe^{III} as the final product (UV-vis spectrum, Figure 1B) in a monophasic reaction, (4).

$$2Fe^{III}Fe^{III} + S_2O_4^{2-} + 2H_2O \rightarrow 2Fe^{II}Fe^{III} + 2SO_3^{2-} + 4H^+ \quad (2)$$

$$Fe^{III}Fe^{III} + 2Cr^{II}L \rightarrow Fe^{II}Fe^{II}\cdots Cr^{III}L + Cr^{III}L \quad (3)$$

$$Fe^{III}Fe^{III} + Cr^{II}L \rightarrow Fe^{II}Fe^{III} + Cr^{III}L \quad (4)$$

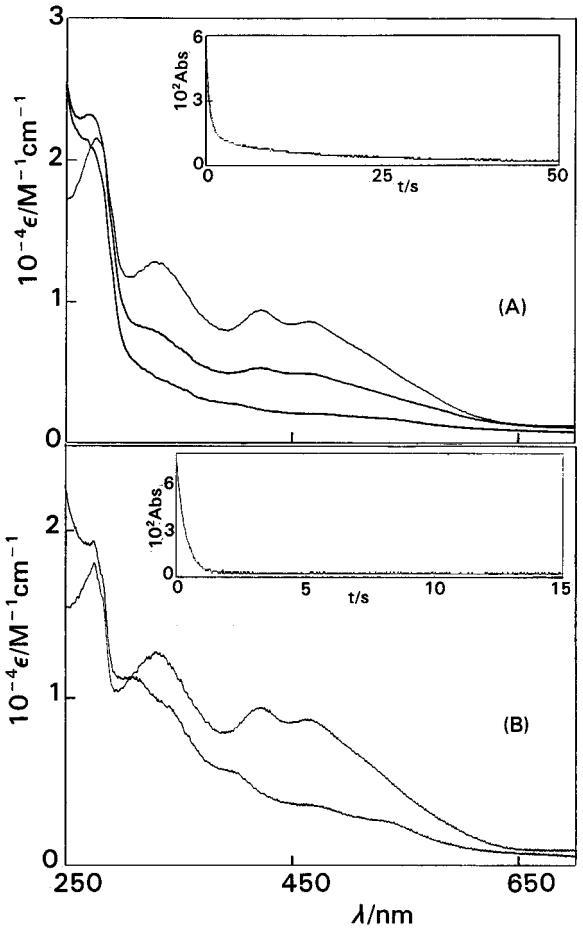

Figure 1. (A) UV−vis spectra for the two-stage 2-equiv reduction of $Fe^{III}Fe^{III}$ spinach FdI (upper trace) by the $Cr^{II}L$ reductant $[Cr(15\text{-ane}N_4)(H_2O)_2]^{2+}$ at pH 7.5 (20 mM Tris/HCl), $I = 0.100$ M (NaCl). The inset shows a stopped-flow trace (25 °C) for the reaction of $Fe^{III}Fe^{III}$ protein (1×10^{-5} M) with $Cr^{II}L$ (0.50 mM), and illustrates the two-phase reaction. (B) UV-vis spectra for the single stage 1-equiv reduction of $Fe^{III}Fe^{III}$ *A. variabilis* FdI (upper trace) by the $Cr^{II}L$ reductant $[Cr(15\text{-ane}N_4)(H_2O)_2]^{2+}$ at pH 7.5 (20 mM Tris/HCl), $I = 0.100$ M (NaCl). The insert is a stopped-flow trace for the reaction (25 °C) of $Fe^{III}Fe^{III}$ protein (1×10^{-5}M) with $Cr^{II}L$ (2.0 mM) and illustrates the single-phase nature of the reaction.

Absorbance changes and kinetics were monitored at 422 nm for the $Cr^{II}L$ (≥15-fold excess) reduction of all three FdI proteins at pH 7.5. Thus two first-order rate constants k_{1obs} and k_{2obs} for spinach and parsley and k_{1obs} only for *A. variabilis* were obtained. Linear dependencies of k_{1obs} and k_{2obs} on $[Cr^{II}L]$ for spinach, Figure 2A (see also listings for parsley and *A. variabilis* in Table 1), are consistent with rate laws as in (5), which define

$$\text{rate} = k[Cr^{II}L][Fe^{III}Fe^{III}] \quad (5)$$

second-order rate constants k, in turn k_1 and k_2. For spinach FdI $k_1 = 2760 \pm 60$ M^{-1} s^{-1} and $k_2 = 660 \pm 20$ M^{-1} s^{-1}, for parsley FdI $k_1 = 1510 \pm 64$ M^{-1} s^{-1} and $k_2 = 210 \pm 19$ M^{-1} s^{-1}, and for *A. variabilis* FdI $k_1 = 1250 \pm 40$ M^{-1} s^{-1}, all at 25 °C, pH 7.5, and $I = 0.100$ M (NaCl).

Reduction of the $Cr^{III}L$-Modified Protein with $Cr^{II}L$. The spinach FdI protein, initially present as $Fe^{III}Fe^{III}\cdots Cr^{III}L$, was reduced with $Cr^{II}L$ (≥50-fold excess) to $Fe^{II}Fe^{II}\cdots Cr^{III}L$. Stopped-flow changes give a biphasic fit with first-order rate constants k_{3obs} and k_{4obs} as listed in Table 2 (Supporting Information). From the dependencies on $[Cr^{II}L]$, Figure 2B, second-order rate constants are $k_3 = 700 \pm 48$ M^{-1} s^{-1} and $k_4 = 115 \pm 90$ M^{-1} s^{-1}. Although a biphasic treatment gives the

(32) Salamon, Z.; Tollin, G. *Bioelectrochem. Bioenerg.* **1992**, *27*, 381.
(33) Knaff, D. B.; Hirasawa, M. *Biochim. Biophys. Acta* **1991**, *1056*, 93.
(34) Cammack, R.; Roa, K. K.; Bargeron, C. P.; Hutson, K. G.; Andrew, P. W.; Rogers, L. J. *Biochem. J.* **1977**, *168*, 205.
(35) Böhme, H.; Schrautemeier, B. *Biochim. Biophys. Acta* **1987**, *891*, 1.
(36) Fujinaga, J.; Gaillard, J.; Meyer, J. *Biochem. Biophys. Res. Commun.* **1993**, *194*, 104.
(37) E.g.: Lambeth, D. O.; Palmer, G. *J. Biol. Chem.* **1973**, *248*, 6095.

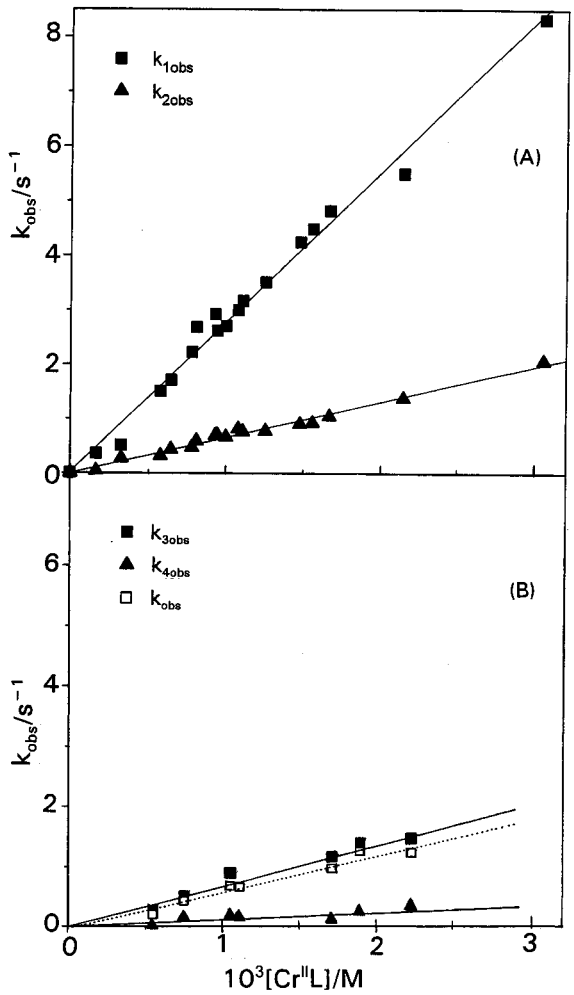

Figure 2. (A) Dependence of first-order rate constants k_{1obs} and k_{2obs} (25 °C) for the biphasic reaction of the $Cr^{II}L$ reductant $[Cr(15\text{-}aneN_4)(H_2O)_2]^{2+}$ (reactant in excess) with $Fe^{III}Fe^{III}$ spinach FdI ($\sim 1 \times 10^{-5}$ M) on concentration of reductant, at pH 7.5 (20 mM Tris/HCl), $I = 0.100$ M (NaCl). (B) Dependence of first-order rate constants k_{3obs} and k_{4obs} (25 °C) for the biphasic reactions of the $Cr^{II}L$ reductant $[Cr(15\text{-}aneN_4)(H_2O)_2]^{2+}$ (reactant in excess) with $Fe^{III}Fe^{III}\cdots Cr^{III}$ spinach FdI ($\sim 1 \times 10^{-5}$ M) on concentration of reductant, at pH 7.5 (20 mM Tris/HCl), $I = 0.100$ M (NaCl). Points for k_{obs} (□) from a uniphasic fit are also shown.

best fit, second-order rate constants $k = 590 \pm 42$ M^{-1} s^{-1} from a uniphasic treatment could also be evaluated. Values of k_3 and k are very similar. We note also that k_3 is similar in magnitude to k_2 (660 M^{-1} s^{-1}) in the previous section.

Effect of $[Cr(en)_3]^{3+}$ on the Reduction with $Cr^{II}L$. Reduction of spinach FdI (1×10^{-5} M) in the $Fe^{III}Fe^{III}$ state with excess $Cr^{II}L$ (1 mM) is inhibited by redox-inactive $[Cr(en)_3]^{3+}$. A biphasic kinetic treatment gives first-order rate constants from which second-order rate constants k_1' and k_2', Table 3 (Supporting Information), are obtained. The dependencies of k_1' and k_2' on $[Cr(en)_3^{3+}]$ are shown in Figure 3. At $[Cr(en)_3^{3+}] > 1.0$ mM, k_1' and k_2' converged, and separate values could no longer be determined with accuracy. From the data at smaller $[Cr(en)_3^{3+}]$, the latter inhibits the k_1' step, but k_2' is unaffected. Assuming that complete blocking of k_1' by $[Cr(en)_3]^{3+}$ occurs (see ref 38), the reaction scheme (6)−(7) is proposed. From

$$Fe^{III}Fe^{III} + [Cr(en)_3]^{3+} \overset{K}{\rightleftharpoons} Fe^{III}Fe^{III}, [Cr(en)_3]^{3+} \quad (6)$$

$$Fe^{III}Fe^{III} + Cr^{II}L \xrightarrow{k_1} Fe^{II}Fe^{III}\cdots Cr^{III}L \quad (7)$$

these, (8) can be derived, and from a graph of $(k_1')^{-1}$ vs $[Cr(en)_3^{3+}]$, $K = 950 \pm 74$ M^{-1} and $k_1 = 2740 \pm 60$ M^{-1} s^{-1}, in close agreement with the value (2760 M^{-1} s^{-1}) already determined. Inclusion of a reaction step involving $Cr^{II}L$

$$k_1' = \frac{k_1}{1 + K[Cr(en)_3^{3+}]} \quad (8)$$

reduction of the adduct formed in (6) gives a rate constant of -260 ± 610 M^{-1} s^{-1}, indicating negligible contribution from this process. The rate constant $k'_2 = 650 \pm 60$ M^{-1} s^{-1} is similar in magnitude to k_2 above (660 M^{-1} s^{-1}) and is not affected by $[Cr(en)_3]^{3+}$. To the right-hand side of Figure 3 the

Table 1. First-Order Rate Constants k_{1obs} and k_{2obs} (25 °C) from a Biphasic Kinetic Treatment for the Reduction of Spinach [2Fe-2S] Ferredoxin I by the $Cr^{II}L$ Reductant $[Cr(15\text{-}aneN_4)(H_2O)_2]^{2+}$ at pH 7.5 (20 mM Tris/HCl), $I = 0.100$ M (NaCl)

$10^3[Cr^{II}L]$/M	k_{1obs}/s^{-1}	k_{2obs}/s^{-1}	$10^3[Cr^{II}L]$/M	k_{1obs}/s^{-1}	k_{2obs}/s^{-1}
Spinach [2Fe-2S] FdI					
0.17	0.36	0.03	1.08	3.02	0.81
0.33	0.51	0.27	1.11	3.17	0.76
0.58	1.51	0.31	1.26	3.51	0.77
0.64	1.71	0.43	1.48	4.30	0.83
0.78	2.22	0.47	1.56	4.49	0.92
0.81	2.68	0.59	1.67	4.80	1.05
0.93	2.92	0.69	2.15	5.50	1.38
0.95	2.62	0.70	3.05	8.33	2.07
1.00	2.70	0.62			
Parsley [2Fe-2S] FdI					
0.51	0.97	0.20	1.25	2.14	0.26
0.89	1.58	0.16	1.63	2.54	0.39
1.11	1.66	0.27	1.71	2.46	0.32
A. variabilis [2Fe-2S] FdI					
0.49	1.50		1.65	2.01	
1.13	1.24		2.19	2.77	

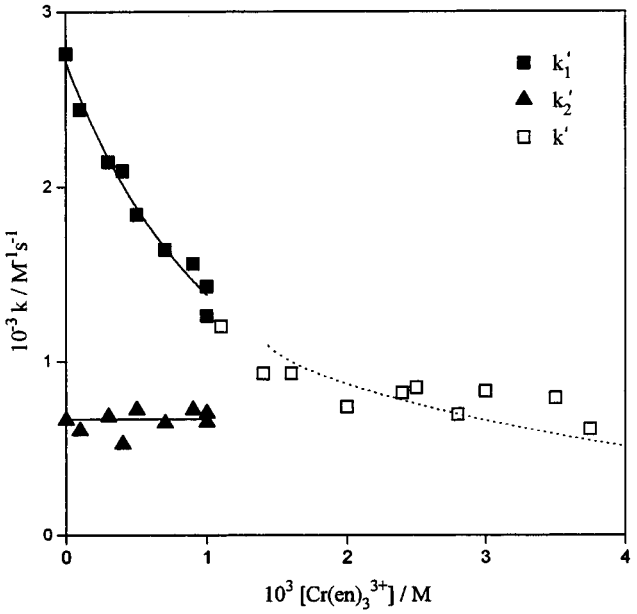

Figure 3. Competitive inhibition by redox-inactive $[Cr(en)_3]^{3+}$ on second-order rate constants k_1' and k_2' (25 °C) for the biphasic reaction of the $Cr^{II}L$ reductant $[Cr(15\text{-}aneN_4)(H_2O)_2]^{2+}$ with $Fe^{III}Fe^{III}$ spinach FdI (1×10^{-5} M) at pH 7.5 (20 mM Tris/HCl), $I = 0.100$ M (NaCl). At the higher concentrations of $[Cr(en)_3]^{3+}$ as k_1' approaches k_2', it was not possible to separate the two stages, and a single rate constant k' (□) is indicated. The best fit to points (■) is extrapolated (---) to higher $[Cr(en)_3^{3+}]$ values using the parameters derived.

(38) Armstrong, F. A.; Henderson, R. A.; Sykes, A. G. *J. Am. Chem. Soc.* **1979**, *101*, 6912.

Table 4. Effect of Redox-Inactive $[Cr(en)_3]^{3+}$ on Second-Order Rate Constants k_3' and k_4' (25 °C) for the Biphasic Reaction of the $Cr^{II}L$ Reductant $[Cr(15\text{-ane}N_4)(H_2O)_2]^{2+}$ (1.0×10^{-3} M) with $Fe^{III}Fe^{III}\cdots Cr^{III}L$-Modified Spinach [2Fe-2S] FdI (2×10^{-5} M) at pH 7.5 (20 mM Tris/HCl), $I = 0.100$ M (NaCl)

$10^3[Cr(en)_3^{3+}]$/M	k_3'/M^{-1} s^{-1}	k_4'/M^{-1} s^{-1}	$10^3[Cr(en)_3^{3+}]$/M	k_3'/M^{-1} s^{-1}	k_4'/M^{-1} s^{-1}
0.00	800	146	1.25	820	194
0.50	750	182	1.75	850	180

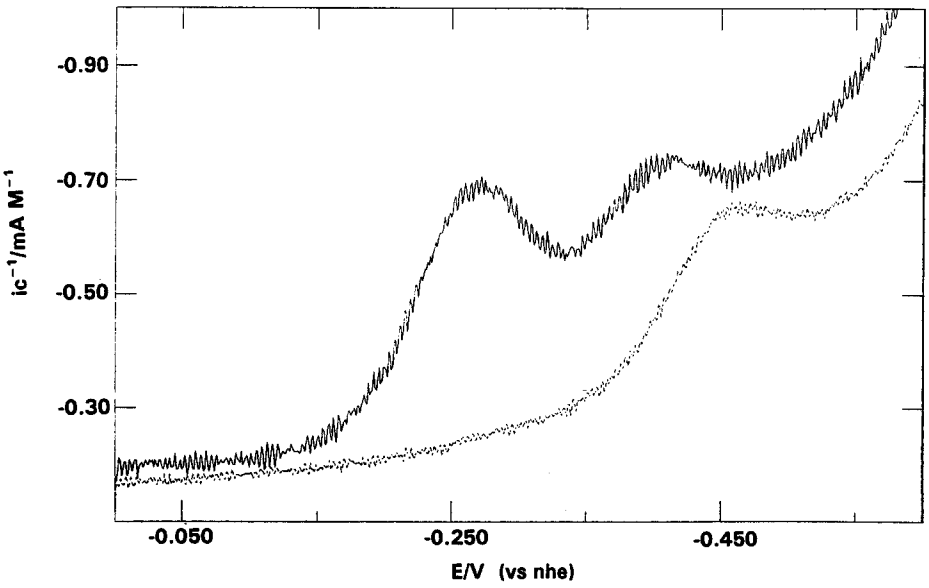

Figure 4. Square-wave voltammetry (25 °C), graph of current (i) over unit of concentration (c) against potential (E vs NHE) for unmodified protein (2.5×10^{-4} M; broken line) and the $Fe^{III}Fe^{III}\cdots Cr^{III}L$ modified form (5×10^{-4} M; solid line) at a gold electrode treated with DEAE-SH promoter, pH 7.5 (20 mM Tris/HCl), $I = 0.100$ M (NaCl).

uniphasic rate constant k becomes less than k_2 but not sufficiently so for the system to revert to two separable rate constants.

Similar experiments were carried out with $Fe^{III}Fe^{III}\cdots Cr^{III}L$ modified spinach FdI as reactant. No inhibition by $[Cr(en)_3]^{3+}$, $(0-1.75) \times 10^{-3}$ M, was observed, Table 4. The two rate constants $k_3 = 805 \pm 107$ M^{-1} s^{-1} and $k_4 = 176 \pm 20$ M^{-1} s^{-1} are similar to those obtained previously (700 M^{-1} s^{-1} and 115 M^{-1} s^{-1}, respectively) with no $[Cr(en)_3]^{3+}$ added.

Electrochemical Studies. Square-wave voltammograms were obtained for native $Fe^{III}Fe^{III}$ protein (one redox stage) and for $Fe^{III}Fe^{III}\cdots Cr^{III}L$ (two redox stages), Figure 4. For the native protein, the peak observed gives a reduction potential of −462 mV vs NHE, which like the value from Salamon and Tollin[32] (−451 mV), is more negative than literature values, −430 mV.[31] The shift may be due to an effect of the promoter. Two well-defined peaks are observed for $Fe^{III}Fe^{III}\cdots Cr^{III}L$ protein (Figure 4) at −273 and −410 mV vs NHE. Both peak heights are the same as for the native protein, suggesting one-electron redox processes. The changes are assigned to the half-reactions (9)−(10)and are consistent with kinetic steps and UV−vis spectrophotometric changes as in Figure 1A.

$$Fe^{III}Fe^{III}\cdots Cr^{III}L + e^- \rightleftarrows Fe^{II}Fe^{III}\cdots Cr^{III}L \qquad (9)$$

$$Fe^{II}Fe^{III}\cdots Cr^{III}L + e^- \rightleftarrows Fe^{II}Fe^{II}\cdots Cr^{III}L \qquad (10)$$

EPR Studies. The EPR spectrum of the $Fe^{II}Fe^{III}$ oxidation state was obtained by reduction of $Fe^{III}Fe^{III}$ protein with excess of dithionite ($g = 1.886$, 1.955, and 2.044), Figure 5A, and is as previously reported.[39,40] On reduction with a ∼1.5-fold amount of $Cr^{II}L$, additional signals at $g =$ ∼1.52, 1.996, and ∼5 are assigned to attached $Cr^{III}L$, Figure 5B. The last signal, not shown in Figure 5, is a broad asymmetric peak ∼45mT wide at half-height. The g values for $Fe^{II}Fe^{III}$ are apparent values and at the precision of the measurements are identical in Figure 5A and Figure 5B. The apparent increase in line width of the signals, in conjunction with a relative lowering of the power saturation, indicates a possible additional influence of the attached $Cr^{III}L$ on the $Fe^{II}Fe^{III}$ signal. Contributions from

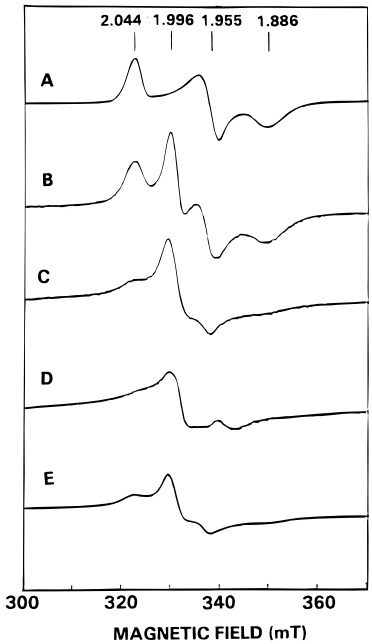

Figure 5. EPR spectra obtained at different gain settings in the $g = 2$ region for spinach FdI (∼0.9 mM): (A) $Fe^{III}Fe^{III}$ proteins reduced to the $Fe^{II}Fe^{III}$ state by 5 equiv of dithionite; (B) $Fe^{III}Fe^{III}$ protein reduced by ∼1.5 equiv of $Cr^{II}L$; (C) $Fe^{III}Fe^{III}$ reduced by a 5-equiv excess of $Cr^{II}L$; (D) $Fe^{III}Fe^{III}\cdots Cr^{III}L$ (0.80 mM) and (E) $Fe^{III}Fe^{III}\cdots Cr^{III}L$ reduced by 5 equiv of $Cr^{II}L$, pH 7.0 (20 mM Tris/HCl), $I = 0.100$ M (NaCl).

(39) Ohmori, D.; Hasimi, H.; Yamakura, F.; Murakami, M.; Fujisaura, K.; Tameoka, Y.; Yamamura, T. *Biochim. Biophys. Acta* **1989**, *996*, 166.
(40) Aliverti, A.; Corrado, M. E.; Zanett, G. *FEBS Lett.* **1994**, *343*, 247.

Table 5. Chemical Shifts (ppm) of ^1H NMR Resonances in Aromatic Residues of Ferredoxins

$Fe^{III}Fe^{III}$ spinach Fd I[a]							$Fe^{III}Fe^{III}$ *A. variabilis* Fd I[b,c]						
residue	H^{β}	H^{δ} (2,6)	H^{ϵ} (3,5)				H^{β}	H^{δ} (2,6)	H^{ϵ} (3,5)				
Tyr-3	2.87,2.74	6.91	6.67										
Tyr-25	3.29,3.1	6.93	6.30				2.7	6.39					
Tyr-35							2.81,2.49	6.80	6.34				
Tyr-39													
Tyr-82	3.18,2.74	6.92	6.32				3.21,2.88	7.13	6.43				
Tyr-99							3.17,2.81	7.13	6.79				
residue	H^{β}	H^{δ} (2,6)	H^{ϵ} (3,5)	H^{ζ} (4)			H^{β}	H^{δ} (2,6)	H^{ϵ} (3,5)	H^{ζ} (4)			
Phe-3							3.30,2.34	7.13	7.21	7.11			
Phe-18	3.40,2.55	6.95	7.05										
Phe-39									7.23	7.34			
Phe-65	3.10,2.80	7.62	7.85	7.76				7.56	7.45	7.35			
residue	H^{β}	H^{δ} (2)	$H^{\epsilon 3}$ (4)	$H^{\zeta 3}$ (5)	$H^{\eta 2}$ (6)	$H^{\zeta 2}$ (7)							
Trp-75	3.35,2.69	7.19	7.68	6.71	7.11	7.32							
residue	H^{β}	$H^{\epsilon 1}$ (2)	$H^{\delta 2}$ (4)				H^{β}	$H^{\epsilon 1}$ (2)	$H^{\delta 2}$ (4)				
His-16							2.57,2.55	7.99	6.89				
His-92	3.19,3.05	7.73	6.92				3.39,3.31	7.81	7.18				

[a] This study; spinach FdI (1.5−2.0 mM), 25 °C, pH 7.1 (50 mM phosphate buffer). [b] Reference 41; *Anabaena* FdI (~3.3 mM), 20 °C, pH 7.2 (50 mM phosphate buffer). [c] Reference 44; *Anabaena* 7120 (6.0−9.0 mM), 25 °C, pH 7.1 (50 mM phosphate buffer).

$Cr^{III}L$ (g = ~1.52, 1.996, and ~5) are similar to those obtained in separate experiments with free $Cr^{III}L$ added (g = ~1.52, 2.149, and ~5). With a 5-fold excess of $Cr^{II}L$, a nearly total decrease in the signals at g = 1.886, 1.955, and 2.044 is observed, Figure 5C, with no noticeable change at g = 1.996. The ~2-fold increase in intensity of the g = ~1.52 and ~5 signals is attributed to the presence of unattached $Cr^{III}L$. The EPR spectrum of $Fe^{III}Fe^{III}$ protein with $Cr^{III}L$ attached, Figure 5D, gives a prominent peak at g = 1.996, which is different from that of a solution of free $Cr^{III}L$. The peak at g = 1.996 is therefore due to $Cr^{III}L$ bound to the protein, where only one $Cr^{III}L$ complex binds in this way in agreement with the ICP-AES analyses. That the decrease in number of peaks is not explained by reoxidation of $Fe^{II}Fe^{III}$ (were this possible) is confirmed by monitoring simultaneously signals assigned to $Cr^{III}L$.

From line-broadening and power saturation studies, a binding site for the $Cr^{III}L$ at a distance of ~15 Å from the cluster is indicated. In addition, the reduction of the Cr^{III}-modified protein, Figure 5D, has been investigated. When a sample of $Fe^{III}Fe^{III}\cdots Cr^{III}L$ protein is reduced with dithionite or $Cr^{II}L$, a decrease in intensity of the signal from $Fe^{II}Fe^{III}$ is observed, Figure 5E, corresponding to formation of $Fe^{II}Fe^{II}\cdots Cr^{III}L$ product. Formation of the latter is not complete in this particular experiment (there is a small residual g = 1.89 signal). No EPR signal is observed for $Fe^{II}Fe^{II}$, and that shown in Figure 5C is directly attributable to the $Cr^{III}L$ component.

NMR Studies. Redox-inactive Cr^{III} complexes, e.g. $[Cr(en)_3]^{3+}$ and $[Cr(NH_3)_6]^{3+}$, behave similarly in blocking the oxidation of $Fe^{II}Fe^{III}$ protein with e.g. $[Co(NH_3)_6]^{3+}$.[38] The site of interaction of $[Cr(NH_3)_6]^{3+}$ with $Fe^{III}Fe^{III}$ protein has been investigated by ^1H NMR and ^{13}C spectroscopy.[41] Selective paramagnetic broadening results indicate that $[Cr(NH_3)_6]^{3+}$ associates (no covalent bonds) with *A. variabilis* FdI at regions close to residues Tyr-25 and Tyr-82 (Tyr-83 in some papers). From X-ray structures,[8−12] the aromatic rings of Tyr-25 and Tyr-82 are stacked. Other studies on *S. maxima* FdII and spinach ferredoxin have been reported.[41] *P. americana* FdI with a Phe-82 occupancy was also found to give line broadening at this position. As an extension of the approach, we were interested in determining the site of attachment of $Cr^{III}L$ to spinach FdI.

Eight aromatic residues on the protein are the prime focus of attention. ^1H resonances were assigned using two-dimen-

(41) Chan, T.-M.; Ulrich, E. L.; Markley, J. L. *Biochemistry* **1983**, *22*, 6002.

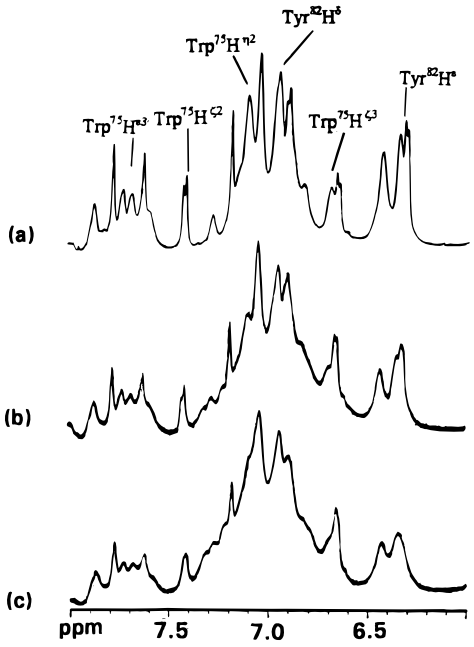

Figure 6. Aromatic region of the ^{1}H NMR spectra (25 °C) of Fe^{III}-Fe^{III} spinach FdI (2 mM): (a) $Fe^{III}Fe^{III}$; (b) $Fe^{III}Fe^{III}\cdots Cr^{III}L$; (c) Fe^{III}-Fe^{III} with 1:15 molar equiv of (unattached) $Cr^{III}L$ at pH 7.0 (20 mM phosphate), $I = 0.100$ M (NaCl).

sional NMR techniques (NOESY and TOCSY). The chemical shifts are listed in Table 5. Previously observed line-broadening effects were confirmed on addition of 1:30 molar ratio of $[Cr(NH_3)_6]^{3+}$ to $Fe^{III}Fe^{III}$ spinach FdI.[41] The resonances (ppm) for Tyr-25 (H^{δ} 6.93 and H^{ϵ} 6.3) and Tyr-82 (H^{δ} 6.92 and H^{ϵ} 6.32) are similarly broadened by 1:15 ratios of unattached $Cr^{III}L$ to protein. The effect of increasing concentrations of $Cr^{III}L$ from 1:15 to 1:3 ratios was also studied. No broadening of other aromatic resonances (Tyr-3, Tyr-39, Phe-18, Phe-65, and His-92) was observed, but substantial broadening of the Trp-75 peaks (ppm) (H^{δ} 7.19, $H^{\epsilon 3}$ 7.68, $H^{\zeta 3}$ 6.71, $H^{\eta 2}$ 7.11, and $H^{\zeta 2}$ 7.32) was noted at the higher concentrations of $Cr^{III}L$ (1:3). This residue is ~11 Å from the $Fe^{III}Fe^{III}$ ferredoxin (β-carbon of residue 75 to Fe_A) but has not so far been considered relevant in electron-transfer studies.[41]

Figure 6 shows the spectrum of $Fe^{III}Fe^{III}\cdots Cr^{III}L$ spinach FdI in the aromatic region of the ^{1}H NMR. The spectrum shows that all the above peaks are more extensively broadened as is to be expected with 1:1 amounts of $Cr^{III}L$ present and as compared to the spectrum of native spinach FdI with free $Cr^{III}L$. Line-broadening effects were also determined with mixtures of native and $Fe^{III}Fe^{III}\cdots Cr^{III}L$ spinach FdI. Peak widths in the aromatic region of these spectra were determined using a line-deconvolution program, and the peak widths at half-height are listed in Table 6. Spectra obtained for the Cr^{III}-modified protein are too broad to measure the widths very accurately. However the change in width of the Tyr-82 resonance for H^{ϵ} is ~9 Hz using a 3:1 ratio of native:$Fe^{III}Fe^{III}\cdots Cr^{III}L$-modified protein, and in the case of Trp-75 ($H^{\epsilon 3}$ and $H^{\zeta 3}$) the differences are 5−7 Hz.

Discussion

The redox properties of three FdI proteins from spinach, parsley, and *A. variabilis* have been explored in this work. Separation of FdI from FdII protein by hydrophobic interaction column chromatography is an essential part of the studies, thus eliminating any spurious FdII contributions to the two-stage kinetic behavior observed with spinach and parsley $Fe^{III}Fe^{III}$. Most emphasis is on the reactivity of spinach FdI. The use of

Table 6. Line Broadening of ^{1}H NMR Resonances (25 °C) in the Aromatic Region of Spinach FdI as $Fe^{III}Fe^{III}$ and as $Cr^{III}L$-Modified $Fe^{III}Fe^{III}\cdots Cr^{III}L$ and of Mixtures As Indicated at pH 7.5 (20 mM Phosphate), $I = 0.100$ M (NaCl)

		peak width at half-height/Hz[b]			
no.[a]	δ/ppm	FdI	9:1 FdI:FdI−$Cr^{III}L$	3:1 FdI:FdI−$Cr^{III}L$	FdI−$Cr^{III}L$
1	7.87	19.3	20.6	20.7	27.5
2	7.77	7.0	8.6	8.8	14.4
3	7.73	20.6	18.8	21.1	30.4
4	7.68	25.3	26.7	30.0	47.4
5	7.62	6.7	7.3	9.0	20.0
6	7.42	7.5	9.5	8.5	11.8
7	7.41	5.5	8.0	8.4	12.1
8	7.19	6.2	6.2	7.1	
9	6.71	23.4	27.8	30.1	37.2
10	6.66	11.7	9.8	10.9	12.9
11	6.44	25.7	24.8	24.8	29.3
12	6.35	21.3	26.3	24.8	26.6
13	6.32	11.3	16.9	20.7	36.7
14	6.30	10.7	17.0	20.0	36.7

[a] Key: (3) His-92 $H^{\epsilon 1}$; (4) Trp-75 $H^{\epsilon 3}$; (5) Phe-65 H^{ϵ}; (6) Trp-75 $H^{\zeta 2}$; (8) Trp-75 H^{δ}; (9) Trp-75 $H^{\epsilon 3}$; (10) Tyr-3 H^{ϵ}; (13) Tyr-82 H^{ϵ}; (14) Tyr-25 H^{ϵ}. [b] Determined by line deconvolution.

$Cr^{II}L$ as reductant is rather special, since absorbance changes, Figure 1A, indicate that the reaction proceeds further than the $Fe^{II}Fe^{III}$ stage. This contrasts with the behavior observed with dithionite as reductant.[42] The final UV-vis spectrum obtained after consumption of 2 equiv of $Cr^{II}L$ is shown in Figure 1A. There is no contribution of $Cr^{II}L$ or $Cr^{III}L$ to observed spectra. Whatever $Cr^{II}L$ concentration is employed, the product isolated after air oxidation and DE52 ion-exchange chromatography is $Fe^{III}Fe^{III}\cdots Cr^{III}L$, with only one $Cr^{III}L$ attached. It is concluded that the second $Cr^{II}L$ reduction is of the "outer-sphere" type with no Cr^{III} attachment resulting.

From the biphasic kinetic treatment described, second-order rate constants (25 °C) for the reaction of spinach FdI with $Cr^{II}L$ are $k_1 = 2760$ M^{-1} s^{-1} and $k_2 = 660$ M^{-1} s^{-1} at pH 7.5. Similar behavior is observed for parsley FdI ($k_1 = 1510$ M^{-1} s^{-1} and $k_2 = 210$ M^{-1} s^{-1}) at pH 7.5, but *A. variabilis* FdI gives only the first stage of reaction ($k_1 = 1250$ M^{-1} s^{-1}) and no $Cr^{III}L$ binding is observed. This is significant, suggesting that, whichever amino acid or acids $Cr^{II}L$ binds to in the case of spinach and parsley FdI, the same or a similar amino acid is not available on *A. variabilis* FdI, a point we return to later. Variations of pH from 8.5 to 5.0 give a >10-fold increase in both k_1 and k_2, but we have not explored this effect in any detail.

The product of the second stage of reduction is assigned the formula $Fe^{II}Fe^{II}\cdots Cr^{III}L$. Reoxidation with $[Co(NH_3)_6]^{3+}$ is rapid, and within a 40 min period some 80% of the original $Fe^{III}Fe^{III}$ absorbance is restored. There is however a slow denaturation of both the spinach and parsley $Fe^{II}Fe^{II}$ forms, which may in part be due to air ingress and sensitivity, as is observed also for the $Fe^{II}Fe^{III}$ protein. In other experiments, it was demonstrated that the $Fe^{II}Fe^{III}$ protein obtained by $S_2O_4^{2-}$ reduction (no $Cr^{III}L$ attached) is not further reduced by $Cr^{II}L$. However dithionite is able to reduce $Fe^{II}Fe^{III}\cdots Cr^{III}L$, the product of the first stage of $Cr^{II}L$ reduction. The presence of attached $Cr^{III}L$ is therefore an essential component for the second stage of reduction to occur. These various observations are summarized in the scheme of Figure 7.

From square-wave voltammetry on column-purified spinach $Fe^{III}Fe^{III}\cdots Cr^{III}L$ reduction potentials of −273 mV ($E_1°'$) and −410 mV ($E_2°'$) vs NHE were obtained. Two separate one-

(42) Mayhew, S. G.; Petering, D.; Palmer, G.; Foust, G. P. *J. Biol. Chem.* **1969**, *244*, 2830.

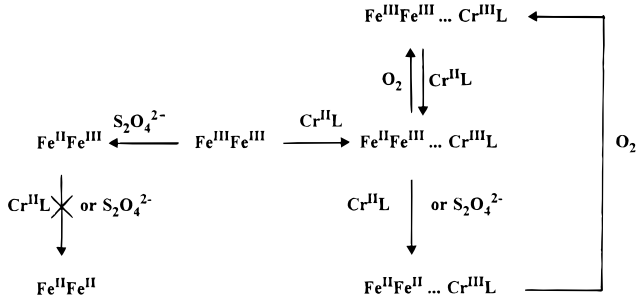

Figure 7. Reaction scheme showing the reactivity of spinach and parsley FdI. *A. variabilis* FdI gives no reaction past the $Fe^{II}Fe^{III}$ state, and no $Cr^{III}L$ is attached.

electron transfer steps are assigned to the $Fe^{III}Fe^{III}Cr^{III}L/Fe^{II}$-$Fe^{III}Cr^{III}L$ (−273 mV) and $Fe^{II}Fe^{III}Cr^{III}L/Fe^{II}Fe^{II}Cr^{III}L$ (−410 mV) couples, respectively. Therefore, attached $Cr^{III}L$ decreases the reduction potential of native spinach FdI (−462 mV) by a very substantial amount—as much as 189 mV—or, on the basis of the literature $E^{\circ\prime}$ (−430 mV), by some 157 mV. This is the first time that the $Fe^{II}Fe^{II}$ ferredoxin state has been generated by chemical or electrochemical means. However special conditions hold in that the attached $Cr^{III}L$ plays an essential role. Comparisons with the behavior of the water-soluble fragment of bovine heart Rieske's [2Fe-2S] protein, which has two His residues coordinated instead of two Cys to one of the Fe atoms, are also relevant. The first reduction potential is unusually high at ∼300 mV.[43] A further redox transition was recently reported to give the superreduced $Fe^{II}Fe^{II}$ form at −840 mV vs NHE.[44]

The chemistry described has been confirmed by EPR spectroscopy. In these studies, a spectrum of $Fe^{III}Fe^{III}$ with $Cr^{III}L$ attached is obtained, which is not the same as that for the $Cr^{III}L$ complex or that for the $Fe^{III}Fe^{III}$ protein in the presence of $Cr^{III}L$, indicating that the $Cr^{III}L$ is in a different environment. On comparison of the g values for $Cr^{III}L$ in the three cases, $Fe^{III}Fe^{III}$ with unattached $Cr^{III}L$, $Fe^{III}Fe^{III}\cdots Cr^{III}L$, and Fe^{II}-$Fe^{II}\cdots Cr^{III}L$, signals at $g = \sim 1.5$ and ∼5 are observed in addition to a derivative type signal at $g = \sim 2$, and the shapes and numbers of components differ in the three instances.

Extensive NMR studies have been carried out by Chan et al.[41] on $Fe^{III}Fe^{III}$ ferredoxins in the presence of $[Cr(NH_3)_6]^{3+}$. Selective broadening of resonances assigned to Tyr-25 and Tyr-82 was observed. The complex $[Cr(CN)_6]^{3-}$ had no similar effect even at concentrations of >1:5 molar equiv, and it was concluded that $[Cr(NH_3)_6]^{3+}$ associates close to the aromatic rings of Tyr-25 and Tyr-82. In addition, the physiological partner ferredoxin-$NADP^+$ oxidoreductase and $[Cr(NH_3)_6]^{3+}$ have been shown to bind competitively and therefore interact at the same site.

The NMR studies carried out as part of the present work were aimed at determining the point of attachment of $Cr^{III}L$. Some broadening of the Tyr-82 resonance in particular was observed, and there is evidence therefore that this residue is attached at or near the same site. However other resonances were broadened also and the effects observed were less specific, most likely due to the relatively high ratio of $Cr^{III}L$ present. An interesting feature of the Tyr-25/Tyr-82 binding site is the number of conserved negatively charged residues in close proximity, Figure 8. Attention has been drawn[45] to the importance of Asp-22, Asp-23, and Asp-62, but there are others,

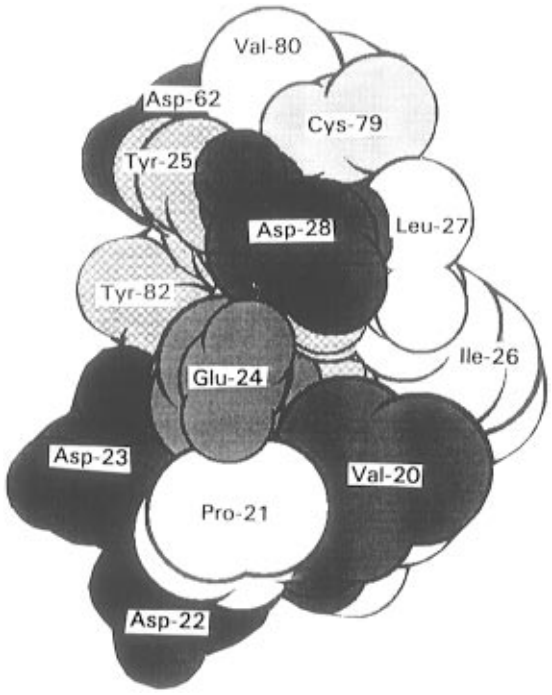

Figure 8. Space-filling model from coordinates for the $Fe^{III}Fe^{III}$ *A. variabilis* FdI structure,[10a] showing the surface Tyr-82/Tyr-25 and acidic patch region, as well as residue 20, in this structure Val but for spinach and parsley Cys.

```
                 10          20          30          40  *   *  *50
(a)  AA YKVTLVT-  PTG-NVEFQC  PDDVYILDAA  EEEGIDLPYS  CRAGSCSSCA
(b)  AT YKVTLVT-  PSG-SQVIEC  GDDEYILDAA  EEKGMDLPYS  CRAGACSSCA
(c)  AT YNVKLIT-  PDG-EVEFKC  DDDVYVLDQA  EEEGIDIPYS  CRAGSCSSCA
(d)  AT FKVKLINE  AEGTKHEIEV  PDDEYILDAA  EEQGYDLPFS  CRAGACSTCA
          ^                    ^^   ^^ ^  ^^   ^ ^ ^  ^^^^ ^^ ^^

                60          70          *80         90
(a)  GKLKTGSLNQ   DDQSFLDDDQ  IDEGWVLTCA  AYPVSDVTIE  THKEEELTA
(b)  GKVTSGSVDQ   SDQSFLEDGQ  MEEGWVLTCI  AYPTGDVTIE  THKEEELTA
(c)  GKVVSGSIDQ   SDQSFLDDEQ  MDAGYVLTCH  AYPTSDVVIE  THKEEEIV
(d)  GKLVSGTVDQ   SDQSFLDDDQ  IEAGYVLTCV  AYPTSDVVIQ  THKEEDLY
     ^    ^  ^    ^^^^^ ^ ^     ^ ^^^^   ^^^  ^       ^^ ^^
```

Figure 9. Amino acid sequences for [2Fe-2S] ferredoxins relevant to this study. Coordinated cysteines (*) and conserved residues (^) are indicated: (a) spinach FdI; (b) spinach FdII; (c) parsley FdI; (d) *A. variabilis* FdI.

namely the conserved acidic residue at 28 (as well as those at 31 and 32) in the same locality, Figure 8. This region of surface has therefore all the requisites of a functionally important site for reaction with cationic reductants.

The results obtained with *A. variabilis* FdI suggest that the residue to which $Cr^{III}L$ is attached is no longer available on this protein. From a comparison of amino acids close to Tyr-25/Tyr-82 including 20−28, 59−62, and 79−84, Figure 9, only two residues on spinach, parsley, and *A. variabilis*, namely Cys, Cys, Val (residue 20) and Val, Val, Glu (residue 24), respectively, show the sort of changes required to explain the different reactivities observed with $Cr^{II}L$. In their studies on *A. variabilis* ferredoxin, Chan et al.[41] suggested the possible involvement of Glu-24 as a site for association. However, we can exclude this position as the site for $Cr^{II}L/Cr^{III}L$ (covalent) binding on spinach and parsley FdI, since the valine residue at position 24 has an inactive side chain $CH_2CH(CH_3)_2$. On the other hand, the Cys at 20 could provide such a site for $Cr^{II}L/Cr^{III}L$ binding in the case of spinach and parsley FdI. The distance to the active site is of interest. No crystal structure information is available for a Cys-20 containing [2Fe-2S] protein, but from the through-bond-pathways program,[46] the distance of a CH_3 of Val-20 to the active-site S atom of Cys-79 is ∼12.8 Å in the *A. variabilis*

(43) Leigh, J. S.; Erecinska, M. *Biochim. Biophys. Acta* **1975**, 95.
(44) Verhagen, M. F. J. M.; Link, T. A.; Hagen, W. R. *FEBS Lett.* **1995**, *361*, 75.
(45) Oh, B.-H.; Markley, J. L. *Biochemistry* **1990**, *29*, 3993.

structure.[10] Since there is reasonable agreement with the ~15 Å from EPR studies, this residue has to be considered as a strong candidate.[47] However the attached $Cr^{III}L$ does have a significant effect on redox properties of the active site, and although two cysteines are interposed between the Cr and Fe, the effect is quite remarkable. Such effects require better understanding in the context of multisite metalloprotein systems.

In kinetic studies, it was shown that $Fe^{III}Fe^{III}\cdots Cr^{III}L$ can be reduced to $Fe^{II}Fe^{II}\cdots Cr^{III}L$ by 2 equiv of $Cr^{II}L$ (k_3 and k_4). The rate constant k_3 is appreciably smaller than k_1, and not surprisingly the attached $Cr^{III}L$ impedes reaction. However, k_3 (700 M^{-1} s^{-1}) is similar in magnitude to k_2 (660 M^{-1} s^{-1}), suggesting that the second site at which $Cr^{II}L$ reduces Fe^{II}-$Fe^{III}\cdots Cr^{III}L$ may be involved also in the reduction of Fe^{III}-$Fe^{III}\cdots Cr^{III}L$. This suggestion gains further support from studies in the presence of redox-inactive $[Cr(en)_3]^{3+}$ as a competitive inhibitor for $Cr^{II}L$.

The first stage of reaction (k_1) appears to undergo complete blocking by $[Cr(en)_3]^{3+}$, as has been observed previously in the oxidation of $Fe^{II}Fe^{III}$ (spinach and parsley) by six oxidants: $[Co_2(NH_3)_{10}(\mu\text{-}NH_2)]^{5+}$, $[Pt(NH_3)_6]^{4+}$, $[Co(NH_3)_6]^{3+}$, $[Cr(phen)_3]^{3+}$, $[Co(NH_3)_5Cl]^{2+}$, and $[Co(NH_3)_5(C_2O_4)]^{+}$.[18,38,48] It has been demonstrated that $[Cr(en)_3]^{3+}$, like $[Cr(NH_3)_6]^{3+}$, associates at the Tyr-25/Tyr-82 site. Whereas k_1 is inhibited by $[Cr(en)_3]^{3+}$, k_2 is unaffected. As the experimentally measured k_1' and k_2' values converge, their separate determinations become more difficult. However, the constant for association of $[Cr(en)_3]^{3+}$ with $Fe^{III}Fe^{III}$ spinach FdI obtained in this study ($K = 950$ M^{-1}) is similar to values previously reported for association of both $[Cr(en)_3]^{3+}$ and $[Cr(NH_3)_6]^{3+}$ with the $Fe^{II}Fe^{III}$ spinach and parsley forms (600−1000 M^{-1}).[18,38] The redox behavior observed clearly indicates therefore two surface sites for reaction. Furthermore, on $Cr^{II}L$ re-reduction of $Fe^{III}Fe^{III}\cdots Cr^{III}L$, addition of $[Cr(en)_3]^{3+}$ has no effect on either k_3 or k_4, which again can be understood in terms of $Cr^{III}L$ (covalently attached) taking the site at which $[Cr(en)_3]^{3+}$ would otherwise associate. $[Cr(en)_3]^{3+}$ does not associate strongly at the second site at which $Cr^{II}L$ reacts. This suggests that a more neutral hydrophobic site is involved. The identity of the second site is at this stage speculation, but one attractive possibility is clearly the surface close to the active site where Cys-41 and Cys-46 are partly solvent exposed. This site will be a target for future site-directed mutagenesis studies.

In conclusion, the present studies with $Cr^{II}L$ as reductant provide the first evidence for reduction of [2Fe-2S] ferredoxins to the $Fe^{II}Fe^{II}$ state. An essential requirement for $Fe^{II}Fe^{II}$ to be generated is that the $Cr^{III}L$ product remains bound to the protein. The site at which the $Cr^{III}L$ is attached appears to be close to Tyr-25/Tyr-82 at a site previously established as a region where cationic inorganic complexes and the physiological oxidoreductase associate. Cysteine-20, present in the case of spinach and parsley FdI (but not *A. variabilis*), appears to be a strong possibility as the point of attachment of $Cr^{III}L$. Evidence for a second site on Fd at which $Cr^{II}L$ reduction occurs has been obtained, but in this case the $Cr^{III}L$ product does not become attached to the protein. The identification of different "in" and "out" sites for electron transfer on [2Fe-2S] ferredoxin, as in the case of plastocyanin, is a possible further outcome of this work.

Acknowledgment. We are grateful to the British Council for a scholarship (to S.-C.I.), and for travel funds under the Alliance Scheme.

Supporting Information Available: Listings of rate constants, Tables 2 and 3 (2 pages). Ordering information is given on any current masthead page.

IC9608253

(46) E.g.: Beratan, D. N.; Onuchic, J. N.; Betts, J. N.; Bowler, B. E.; Gray, H. B. *J. Am. Chem. Soc.* **1990**, *112*, 7915.

(47) In further on-going studies on the $Cr^{II}L$ reduction of maize [2Fe-2S], which has no cysteine at position 20, only a single stage reduction is observed, and there is no $Cr^{III}L$ attachment (Worrall, J. A. R; Hase, T.; Akashi, T.; Sykes, A. G, unpublished work).

(48) Armstrong, F. A.; Sykes, A. G. *J. Am. Chem. Soc*. **1978**, *100*, 7710.